[CANCER RESEARCH 64, 4629–4636, July 1, 2004]

In Vitro and *in Vivo* Activity of the Maytansinoid Immunoconjugate huN901-$N^{2'}$-Deacetyl-$N^{2'}$-(3-Mercapto-1-Oxopropyl)-Maytansine against $CD56^+$ Multiple Myeloma Cells

Pierfrancesco Tassone,[1,2,3] Antonella Gozzini,[1] Victor Goldmacher,[4] Masood A. Shammas,[2] Kathleen R. Whiteman,[4] Daniel R. Carrasco,[1] Cheng Li,[1] Charles K. Allam,[2] Salvatore Venuta,[3] Kenneth C. Anderson,[1] and Nikhil C. Munshi[1,2]

[1]Jerome Lipper Multiple Myeloma Center, Dana-Farber Cancer Institute, and [2]VA Boston Healthcare System, Harvard Medical School, Boston, Massachusetts; [3]University of "Magna Græcia", Catanzaro, Italy; and [4]ImmunoGen, Inc., Cambridge, Massachusetts

ABSTRACT

HuN901 is a humanized monoclonal antibody that binds with high affinity to CD56, the neuronal cell adhesion molecule. HuN901 conjugated with the maytansinoid $N^{2'}$-deacetyl-$N^{2'}$-(3-mercapto-1-oxopropyl)-maytansine (DM1), a potent antimicrotubular cytotoxic agent, may provide targeted delivery of the drug to CD56 expressing tumors. Based on gene expression profiles of primary multiple myeloma (MM) cells showing expression of CD56 in 10 out of 15 patients (66.6%) and flow cytometric profiles of MM ($CD38^{bright}CD45^{lo}$) cells showing CD56 expression in 22 out of 28 patients (79%), we assessed the efficacy of huN901-DM1 for the treatment of MM. We first examined the *in vitro* cytotoxicity and specificity of huN901-DM1 on a panel of $CD56^+$ and $CD56^-$ MM cell lines, as well as a $CD56^-$ Waldenstrom's macroglobulinemia cell line. HuN901-DM1 treatment selectively decreased survival of $CD56^+$ MM cell lines and depleted $CD56^+$ MM cells from mixed cultures with a $CD56^-$ cell line or adherent bone marrow stromal cells. *In vivo* antitumor activity of huN901-DM1 was then studied in a tumor xenograft model using a $CD56^+$ OPM2 human MM cell line in SCID mice. We observed inhibition of serum paraprotein secretion, inhibition of tumor growth, and increase in survival of mice treated with huN901-DM1. Our data therefore demonstrate that huN901-DM1 has significant *in vitro* and *in vivo* antimyeloma activity at doses that are well tolerated in a murine model. Taken together, these data provide the framework for clinical trials of this agent to improve patient outcome in MM.

INTRODUCTION

Recent advances in monoclonal antibody (mAb) technology including humanization and mAb engineering have facilitated the use of mAbs to treat human cancers with enhanced antitumor activity (1, 2). These mAbs selectively target tumor tissues (3–5) and have been safely administered in cancer patients. The recent approvals of mAbs for clinical use (1, 2) have renewed interest in mAb-based therapies.

The direct linking of mAbs with drugs, toxins, or radionuclides to specifically target cancer cells has been widely studied (6). However, the use of mAbs to deliver therapeutic doses of conventional cytotoxic drugs, including doxorubicin, methotrexate, and *Vinca* alcaloids, has led to only limited benefit (7–9). mAbs conjugated to protein toxins, such as ricin or *Pseudomonas* toxin, are highly active *in vitro* and are selective, unlike corresponding unconjugated toxins (6, 10). However, *in vivo* these immunotoxins have significant side effects and retain their high immunogenicity. Despite initial disappointing results, there is now a resurgence of interest due to approval of gemtuzumab ozogamicin (Mylotarg; Ref. 11), a humanized anti-CD33 mAb linked to a semisynthetic, highly cytotoxic calicheamicin γ_1 derivative. Gemtuzumab ozogamicin has demonstrated potent antitumor activity in tumor xenograft models of myeloid leukemia in athymic mice (12) and in patients with $CD33^+$ myeloid leukemia (13). Maytansine derivatives represent a new class of highly cytotoxic agents suitable for conjugation with mAbs. Maytansine (14) is a natural product, originally derived from the Ethiopian shrub *Maytenus serrata*, which inhibits tubulin polymerization, thereby resulting in mitotic block and cell death. The activity of maytansine is approximately 200–1,000-fold greater than that of the *Vinca* alkaloids, which exert their cytotoxic potential by a similar mechanism. Maytansine has shown some activity in clinical studies (15–18), but its narrow therapeutic window precluded additional clinical development. A recently developed highly cytotoxic maytansine derivative $N^{2'}$-deacetyl-$N^{2'}$-(3-mercapto-1-oxopropyl)-maytansine (DM1; Ref. 19) has been linked to the mAb huC242. This antibody targets a glycotope (CanAg) on MUC1 that is expressed on human colorectal and pancreatic tumors (20). After preclinical evaluation (21), a Phase I study of huC242-DM1 in chemotherapy-refractory patients confirmed biological activity in the absence of severe toxic effects (22). Based on these encouraging results, a maytansinoid immunoconjugate with the humanized anti-CD56 mAb, huN901, has been generated for the treatment of CD56-expressing tumors.

CD56 antigen, identified as neuronal cell adhesion molecule (NCAM; Ref. 23), is a membrane glycoprotein belonging to the immunoglobulin superfamily. In the hematopoietic compartment, CD56 expression is restricted to NK cells and a subset of T lymphocytes (24, 25) that specifically express the M_r 140,000 isoform of NCAM glycoprotein (26). The expression of CD56 has also been detected on a variety of cancer cells of hematopoietic and neuroendocrine origin, including multiple myeloma (MM), leukemia, neuroblastoma, and small cell lung carcinoma (SCLC; Refs. 27 and 28). Although normal plasma cells (PCs) do not express CD56 (29), it is expressed by a subset of PCs in patients with monoclonal gammapathy of undetermined significance and strongly expressed on MM cells (29, 30) from a majority of MM (31, 32). In contrast, CD56 is absent on malignant PCs from patients with PC leukemia and/or extramedullary plasmacytoma (33–36).

The restricted expression profile of CD56 in the normal hematopoietic compartment, coupled with its expression on malignant PCs, provided the rationale for evaluating CD56 as a potential target for mAb-based therapy in MM. Herein, we report selective *in vitro* cytotoxicity of huN901-DM1 against a panel of $CD56^+$ MM cell lines, MM cells adherent to bone marrow stroma cells (BMSCs), and patient MM cells. We also demonstrate *in vivo* antitumor activity of huN901-DM1 in a tumor xenograft model with human $CD56^+$ MM cells in SCID mice, providing a rationale for its evaluation in MM patients.

Received 1/15/04; revised 3/5/04; accepted 4/26/04.

Grant support: Multiple Myeloma Research Foundation Awards (M. Shammas, N. Munshi, and K. Anderson); VA merit review, and the Leukemia and Lymphoma Society Scholar in Translational Research Award (N. Munshi); NIH Grants RO1-50947, P50-100707, and PO1-78378 (N. Munshi and K. Anderson); the Doris Duke Distinguished Clinical Research Scientist Award (K. Anderson).

The costs of publication of this article were defrayed in part by the payment of page charges. This article must therefore be hereby marked *advertisement* in accordance with 18 U.S.C. Section 1734 solely to indicate this fact.

Requests for reprints: Nikhil C. Munshi, Dana-Farber Cancer Institute, 44 Binney Street (D1B25), Boston, MA 02115. Phone: (617) 632-5607; Fax: (617) 582-7904; E-mail: nikhil_munshi@dfci.harvard.edu.

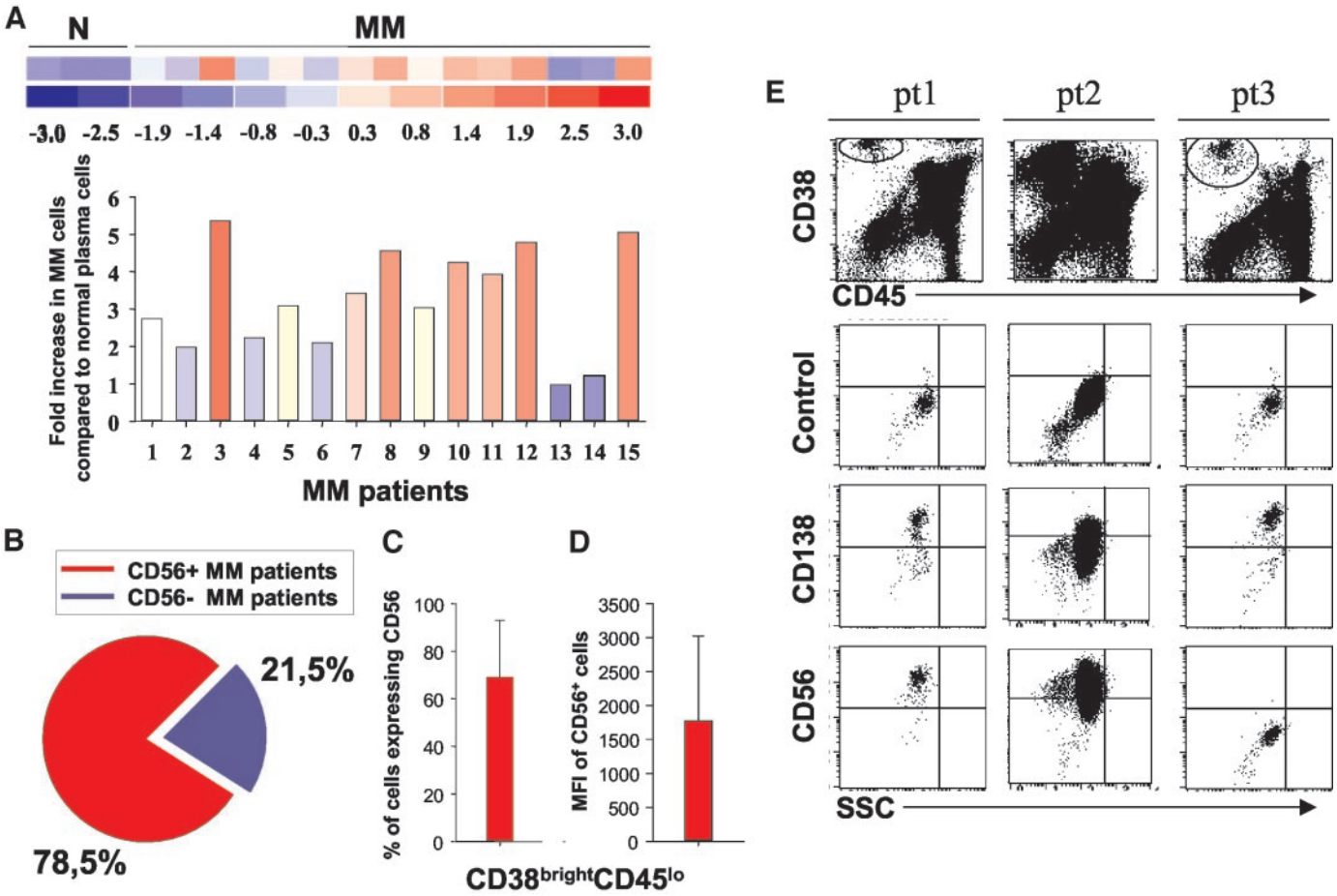

Fig. 1. Expression of CD56 in MM. *A*, CD56 gene expression profile in CD138$^+$ purified (> 95%) normal (three samples) and malignant PCs (15 MM samples); *B*, percentage of patients expressing CD56$^+$ MM cells, as determined by flow cytometry on fresh BM aspirate samples; *C*, percentage (the mean value) of CD56$^+$ cells in fresh BM aspirates taken from 22 CD56$^+$ patients as determined by flow cytometry; *D*, MFI of staining of CD56$^+$ MM cells within CD38^{bright}CD45^{lo} population (a mean value for 22 patients); *E*, flow cytometric profiles of CD56 expression on primary MM cells from patients *pt1*, *pt2*, and *pt3*. CD38^{bright}CD45^{lo} population was assessed for CD56 or CD138 expression within the gate.

MATERIALS AND METHODS

Preparation of mAb-DM1 Conjugate. The thiol-containing maytansinoid DM1 was synthesized from the microbial fermentation product ansamitocin P-3 as described previously (19). Humanized antibodies N901 (huN901) and C242 (huC242) have been described previously (37). Antibody-drug conjugates were prepared as described elsewhere (21). An average of about 3.5 DM1 molecules were linked per antibody molecule.

Cell Lines and Patient Cells. U266 MM cell line was obtained from the American Type Culture Collection (Rockville, MD). OPM1 and OPM2 cell lines were kindly provided by Dr. Edward I. B. Thompson (University of Texas Medical Branch, Galveston, TX); LP1 MM cell line, WSU-Waldenstrom's macroglobulinemia (WM) cell line, and SUDHL4 lymphoma cell line were kindly provided by Dr. P. Leif Bergsagel (Weill Medical College of Cornell University, New York, NY), Dr. Ayad Al-Katib (Wayne State University, Detroit, MI), and Dr. Margaret Shipp (Dana-Farber Cancer Institute, Boston, MA), respectively. Cell lines were cultured in RPMI 1640 (Life Technologies) supplemented with 10% fetal bovine serum (Hyclone, Logan, UT), L-glutamine, penicillin, and streptomycin (Life Technologies) (RPMI complete). PCs and bone marrow (BM) cells were isolated from BM aspirates obtained from MM patients after informed consent for the use of samples for research purpose. BM cells were separated using Ficoll-Hypaque density gradient sedimentation. BMSCs were obtained by long-term cultures of BM cells (4–8 weeks) in RPMI 1640 supplemented with 20% fetal bovine serum.

Gene Expression and Microarray Data Analysis. PCs were isolated from BM aspirate samples of normal donors and patients with MM by positive immunomagnetic bead selection using anti-CD138 antibodies and magnet assisted cell sorting (Miltenyi Biotech). Purity of PCs (> 95%) was assessed by both flow cytometry (Becton-Dickinson FACSort) monitoring the expression of CD38, CD45, and forward and side scatter characteristics of PC or morphological examination.

Total RNA was isolated from 5×10^6 cells using RNeasy kit (Qiagen). Total RNA (10–15 μg) was reverse-transcribed to get cDNA using Superscript II RT kit (Invitrogen). cDNA was used in an *in vitro* transcription reaction to synthesize biotin-labeled cRNA using Enzo RNA labeling kit (Enzo Diagnostics). Labeled cRNA was purified with the RNeasy Mini-kit (Qiagen) and quantitated. Purified cRNA (15 μg) was hybridized to human genome U133 GeneChip arrays (Affymetrix) representing approximately 33,000 human genes. GeneChip arrays were scanned on a GeneArray Scanner (Affymetrix). Normalization of arrays and calculation of expression values were performed using the DNA-Chip Analyzer (dChip) program. Arrays were normalized based on relative signal produced for an invariant subset of genes. This model-based method was used for probe selection and computing expression values.

Colorimetric Survival Assay. Cell survival was examined using a tetrazolium colorimetric assay (CellTiter 96 nonradioactive cell proliferation assay; Promega), as described previously (38). Cells (1×10^4) were plated in 24-well plates in 1 ml of RPMI complete and then treated as indicated. At the end of each treatment, cells were incubated with 150 μl of dye solution and then incubated for 4 h at 37°C. A solubilization/stop solution was then added to each well under vigorous pipetting to dissolve the formazan crystals. Absorbance was measured at 570 nm, and cell viability was estimated as the percentage of untreated controls. All experiments were repeated three times, and each set of experimental conditions was repeated in triplicate wells in each experiment. Data reported are average values ± SD of three representative experiments.

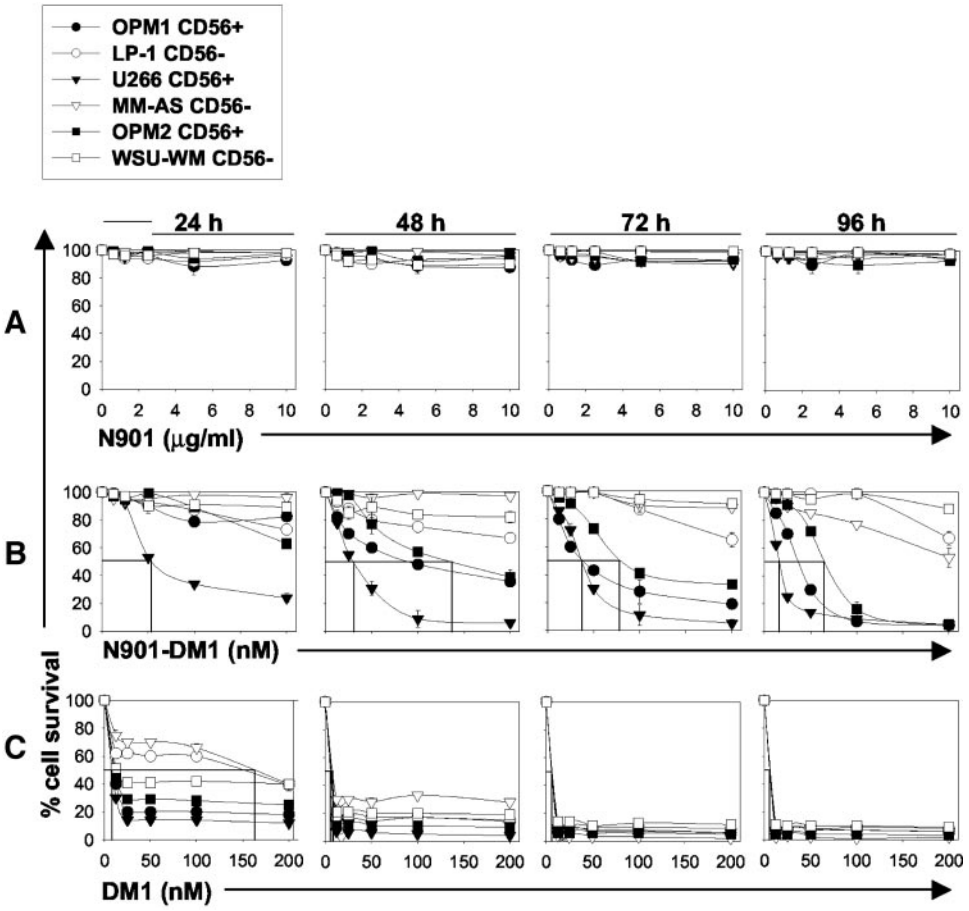

Fig. 2. Effect of huN901-DM1 on survival of $CD56^+$ and $CD56^-$ MM cells. MM cell lines were exposed to unconjugated huN901 mAb (*A*), huN901-DM1 immunoconjugate (*B*), or free DM1 drug (*C*) at equimolar concentrations. Cell survival was measured using an MTT assay. Data (mean ± SD of triplicate experiments) are expressed as percentage of untreated controls. MM cells are *OPM1, OPM2, U266, LP-1*, and *MM-AS*. The WM cell line is *WSU-WM*.

Cell Proliferation Assay. Cell proliferation was measured by the extent of [^{3}H]thymidine (Perkin-Elmer) incorporation. MM cells (2×10^4 cells/well) were incubated in 96-well culture plates in the presence of 70–80% confluent BMSCs at 37°C with or without a test agent (in triplicate wells). [^{3}H]Thymidine (0.5 μCi) was then added for the last 8 h to each well 48-h cultures. Cells were harvested onto glass filters with an automatic cell harvester (Cambridge Technology) and counted using a Micro-β Trilux counter (Wallac).

Cocultures of $CD56^+$ and $CD56^-$ Cells. OPM2 cells and SUDHL4 or WSU-WM cells were plated together at an indicated ratio in 24-well plates in RPM1 1640 supplemented with 10% fetal bovine serum, in the presence or absence of huN901-DM1. Cells were cultured for 72 h with a test agent, and percentages of cells expressing various cell surface antigens were then determined by flow cytometry after staining cells with respective antibodies. Specific cell populations were detected in mixed cultures as $CD138^+$ (OPM2), $CD20^+$ (SUDHL4), and $CD45RA^+$ (WSU-WM). Primary MM cells were detected by double staining using CD56 and CD138 markers. Cell concentrations and viabilities were measured by trypan blue exclusion and hemocytometric cell count.

Detection of Apoptosis. Dual staining with FITC-labeled annexin V and propidium iodide (PI) was carried out to detect induction of apoptotic cell death. After treatment of 1×10^6 cells with a test agent for 48 h, cells were washed with PBS and re-suspended in 100 μl of 4-(2-hydroxyethyl)-1-piperazineethanesulfonic acid (HEPES) buffer containing annexin V-FITC and PI (annexin V-FLUOS staining kit; Roche). After 15 min of incubation at room temperature, cells were analyzed on a Coulter Epics XL flow cytometer for the presence of an annexin V-FITC-positive/PI-negative apoptotic cell population.

Cell Cycle Analysis. MM cells (1×10^6) were incubated with or without a test agent for 48 h, washed with PBS, permeabilized by a 30-min exposure to 70% ethanol at 4°C, incubated with PI (50-μg/ml) in 0.5 ml of PBS containing 20 units/ml RNase A (Roche) for 30 min at room temperature, and analyzed for DNA content by cell-associated fluorescence on a flow cytometer using CellQuest software.

Xenograft Human Tumor Model in SCID Mice. Six-week-old male CB-17 SCID mice (Taconic) were irradiated with 250 cGy and then s.c. inoculated in the interscapular area with 5×10^6 OPM-2 cells in 100 μl of RPMI 1640. In the first series of experiments, mice were treated i.v. with the vehicle alone or with huN901 (13.3 μg/kg) for 5 days. The treatment was initiated after the detection of palpable tumors. Tumor growth was measured weekly in two dimensions using a caliper, and the volume was expressed in mm^3 using the formula $V = 0.5a \times b^2$, where a and b are the long and short diameter of the tumor, respectively. Tumor size was evaluated from the 1st day of treatment until the day of first sacrifice. Animals were sacrificed when their tumors reached 2 cm in diameter to prevent unnecessary suffering. The survival time is defined as the time interval between the start of the experiment and either death or the day when the tumor reached 2 cm in diameter. In the second series of experiments, mice were treated i.v. with vehicle alone, huN901-DM1 (conjugate containing 75 μg DM1/kg/day), or huC242-DM1 (150 μg DM1/kg/day) for a total of 5 days. The treatment was initiated after the detection of measurable levels of human λ chain produced by OPM-2 cells, before the detection of palpable tumors. Detection of paraprotein and huN901-DM1 (IgG1, κ), or huC242-DM1 (IgG1, κ) was achieved using ELISA assays (Bethyl) that selectively detect either human λ or κ chain. The third series of experiments was performed to determine the effect of huN901-DM1 on mice bearing palpable tumors (average size of 200 mm^3). Mice were treated i.v. either with the vehicle alone or with huN901-DM1 (either 75 μg DM1/kg/day or 150 μg DM1/kg/day, respectively), or with huC242-DM1 (150 μg DM1/kg/day), for a total of 5 days. The tumor size and mouse survival were evaluated as above. In addition, two mice bearing very large tumors (average size of 1800 mm^3) were treated with huN901-DM1 (200 μg DM1/kg/day) for a total of 5 days and observed for the changes in the tumor size.

Measurement of Serum Paraprotein Concentration. Blood (50–100 μl) was withdrawn from the tail vein for measurement of human paraprotein in serum by ELISA (Bethyl). Goat antihuman λ and κ antisera were used for capture, and goat antihuman λ or κ horseradish peroxidase conjugates were used for detection.

Statistical Analysis. Statistical significance of differences was determined using Student's t test. Data were considered significant when $P < 0.05$.

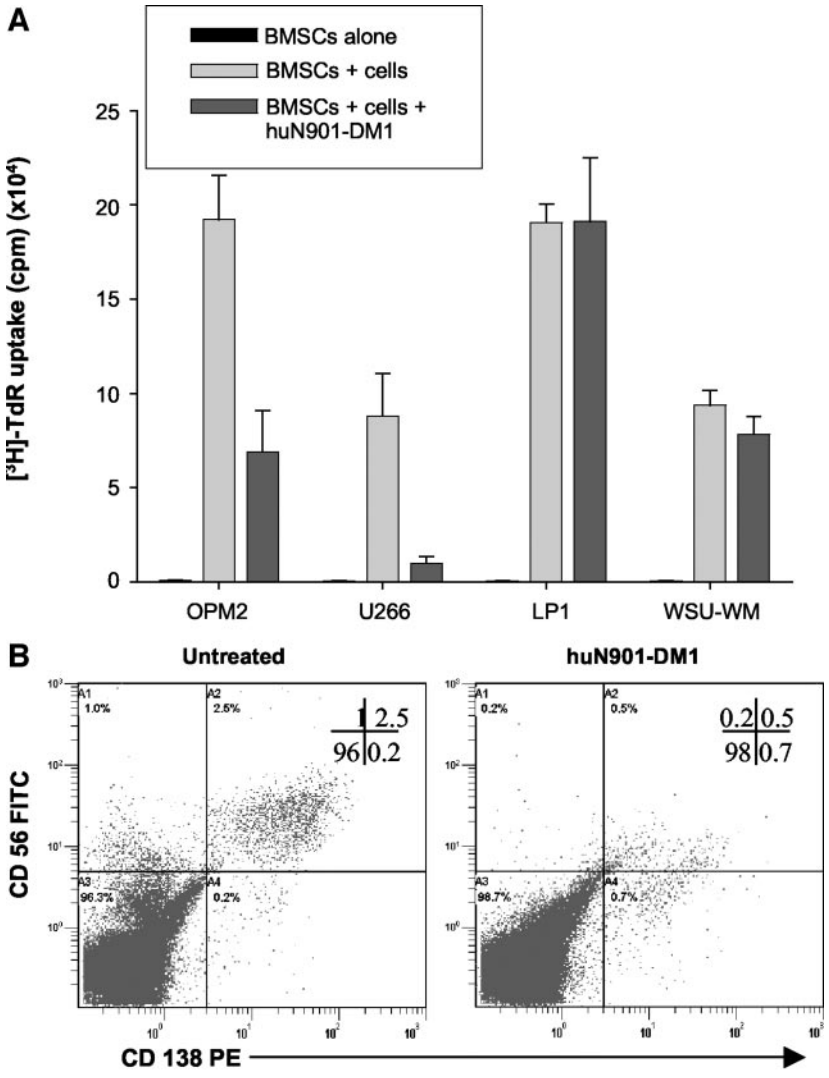

Fig. 3. Inhibitory effect of huN901-DM1 on proliferation of $CD56^+$ and $CD56^-$ cells adherent to BMSCs. *A*, MM or WM cells (2×10^4) were seeded on 70–80% confluent BMSC for 24 h. Cell proliferation was measured by [^{3}H]thymidine (*[^{3}H]-TdR*) incorporation after 72 h of treatment with huN901-DM1 (100 nM). Values represent the mean of [^{3}H]thymidine incorporation (cpm) of triplicate cultures. *B*, primary MM cells were cultured on BMSC layers and exposed for 72 h to the huN901-DM1 immunoconjugate. CD56 and CD138 expression was evaluated with flow cytometry. We have established that huN901-DM1, even at a concentration as high as 50 μM did not affect the binding of the FITC-labeled anti-CD56 antibody (Serotec) to CD56-expressing cells. Figure is representative of two experiments. The number of events (as a percentage of total number of events) for each quadrant is shown in the *top right quadrant*.

RESULTS

Expression of CD56/NCAM in MM Patients. We first measured the CD56 expression on patient MM cells to evaluate the potential utility of CD56 as a target for antibody-based therapy. We analyzed CD56/NCAM gene expression profiles of normal PCs ($n = 3$) and patient MM cells ($n = 15$) using human genome U133 GeneChip array (Affymetrix) data. As seen in Fig. 1*A*, CD56/NCAM was expressed in 10 out of the 15 examined MM specimens (66.6%), at a 3.2-fold mean increase in intensity relative to normal PCs.

We next used flow cytometric data to assess cell surface expression of CD56 on MM cells from 28 patients. Expression of CD56 on $CD38^{bright}CD45^{lo}$ MM cells was determined as the percentage of positive cells and the mean fluorescence intensity (MFI). Twenty-two out of 28 patients (78.5%; Fig. 1*B*) expressed CD56, with a mean of 69 ± 24% $CD56^+$ cells (Fig. 1*C*) and MFI of 1779 ± 1241, (range, 219-4800; Fig. 1*D*). In these cases, the majority of $CD38^{bright}CD45^{lo}$ cells expressed CD56, however a small fraction of cells with low MFI, which also includes normal PC, were considered negative. Fig. 1*E*

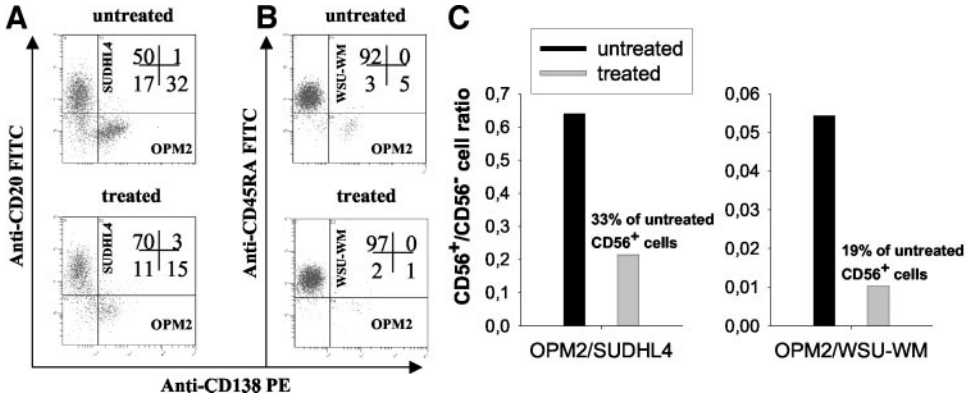

Fig. 4. CD56-specific cytotoxicity of huN901-DM1 in mixed cultures of $CD56^+$ and $CD56^-$ cells. $CD56^+$ OPM2 cells were mixed with $CD56^-$ SUDHL4 at a ratio of 1:2 (*A*) or with WSU-WM cells at a ratio of 1:20 (*B*). Data are from representative experiments. Cells were exposed to 200 nM huN901-DM1. Proportion of MM cells were scored as $CD138^+CD20^-$ or $CD138^+CD45RA^-$ cells, respectively. *C*, $CD56^+/CD56^-$ cell ratio between huN901-DM1 treated and untreated cells.

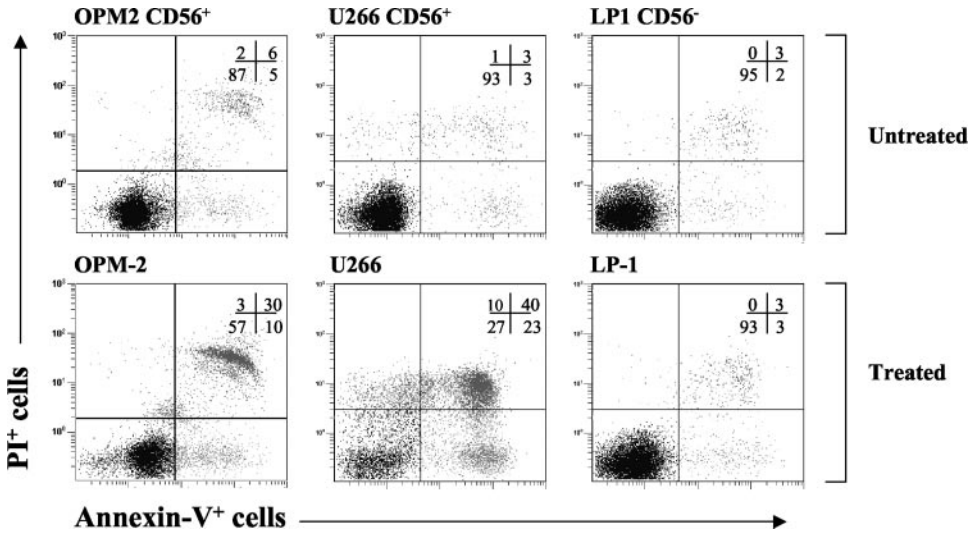

Fig. 5. Induction of apoptotic cell death in $CD56^+$ OPM2 and U266 cells and $CD56^-$ LP-1 MM cells after 48 of exposure to huN901-DM1 (100 nM). Cells were stained with PI and annexin V and then analyzed by flow cytometry. Percentages of stained cells for each quadrant are shown in the *top right quadrant*.

shows three representative profiles of high CD56 expression (pt1 and pt2) or absence of CD56 (pt3) on MM cells. Taken together, these results indicate that CD56 is strongly expressed on a significant fraction of patient MM cells.

HuN901-DM1 Is Selectively Cytotoxic to $CD56^+$ MM Cell Lines *in Vitro*. We next examined the time- and dose-dependent effects of huN901-DM1 on the survival of $CD56^+$ (OPM1, OPM2, and U266) and $CD56^-$ (LP1 and MM-AS) MM cells, as well as $CD56^-$ (WSU-WM) WM cells using an MTT assay. As seen in Fig. 2, treatment with huN901-DM1 (1–200 nM) induced selective growth inhibition in $CD56^+$ tumor cells. This effect was detected at 24 h in U266 cells (IC_{50} = 70 nM), with maximal activity at 96 h in all $CD56^+$ cells (IC_{50} = 10–50 nM). In contrast, huN901-DM1 (1–200 nM) was not toxic to $CD56^-$ MM and WM cells even when treated for 96 h. The sensitivity of these three $CD56^+$ cell lines to the cytotoxic effect of huN901-DM1 (U266 cells were more sensitive than OPM1 or OPM-2; Fig. 2*B*) did not correlate with the order of the level of expression of CD56 on the surface of these cells (U266 ≪ OPM2 ≪ OPM1; data not shown). To confirm that the inhibitory activity of huN901-DM1 is specifically related to mAb-delivered cytotoxicity, we similarly tested the effect of the huN901 antibody and the unconjugated drug DM1. At 96 h, even the highest tested concentrations of huN901 did not affect the growth of MM and WM cells (Fig. 2*A*), whereas DM1 alone was comparably and highly cytotoxic for both $CD56^+$ and $CD56^-$ cell lines (Fig. 2*C*). These data indicate that the cytotoxic effect induced by huN901-DM1 is neither related to the intrinsic properties of the mAb huN901 nor to the differential sensitivity of cells to DM1.

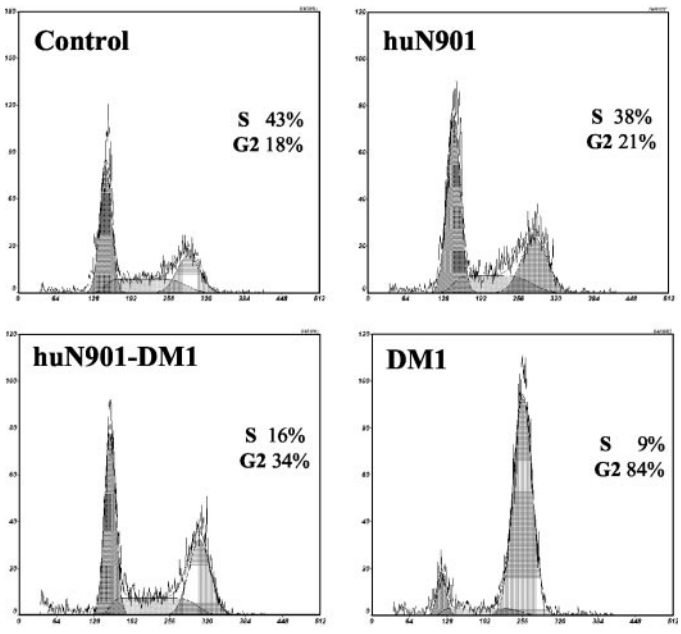

Fig. 6. Effects of huN901-DM1 treatment on cell cycle. OPM2 MM cells were exposed to huN901 mAb, huN901-DM1 immunoconjugate, or free DM1 drug at equimolar concentrations (100 nM) for 48 h. Cell cycle profile was analyzed using PI staining, and percentages of cells in S phase (*S*) and G_2-M (*G2*) phase are indicated in each quadrant. Data are representative of three experiments.

HuN901-DM1 Is Cytotoxic to $CD56^+$ MM Cell Lines and Patient MM Cells Adherent to BMSCs. Because adhesion of MM cells to BMSC protects MM cells from drug-induced apoptosis, we next evaluated the effect of huN901-DM1 on proliferation of $CD56^+$ (OPM2 and U266) and $CD56^-$ (LP1) MM cells and of $CD56^-$ (WSU-WM) WM cells adherent to BMSC. Proliferation was measured by the extent of [^{3}H]thymidine incorporation at 72 h. As seen in Fig. 3*A*, huN901-DM1 (100 nM) markedly inhibited the proliferation of $CD56^+$ OPM2 and U266 cells but had no significant effect on $CD56^-$ cells. Unconjugated DM1 (100 nM) was cytotoxic to all cells (not shown).

We also evaluated the activity of huN901-DM1 (100 nM) on $CD56^+/CD138^+$ patient MM cells cultured with BMSCs (Fig. 3*B*). After 72 h of treatment with huN901-DM1, a greater than 50% reduction in the MM cell population was achieved, which was associated with a decrease in CD138 MFI characteristic of apoptotic MM cell death (39). However, we have been unable to further characterize these cells due to the very low number of remaining cells after the treatment. We further established that binding of CD56 expressing cells with huN901 did not result in down-regulation of CD56 surface expression (data not shown). Taken together, these results indicate that tumor cell adhesion to BMSC does not protect against specific cytotoxicity by huN901-DM1, which overcomes cell adhesion-mediated drug resistance.

HuN901-DM1 Selectively Depletes $CD56^+$ MM Cells in Mixed Cultures with $CD56^-$ Cells. Because huN901-DM1 did not affect $CD56^-$cells ($IC_{50} \leq$ 200 nM), we further evaluated the ability of huN901-DM1 to specifically deplete $CD56^+$ cells cultured together with $CD56^-$ cells. $CD56^+$ OPM2 ($CD138^+/CD20^-$) MM cells were cultured with $CD56^-$ SUDHL4 cells ($CD138^-/CD20^+$) at a ratio of 1:2 or with $CD56^-$ WSU-WM cells ($CD138^-/CD45RA^+$) at a ratio

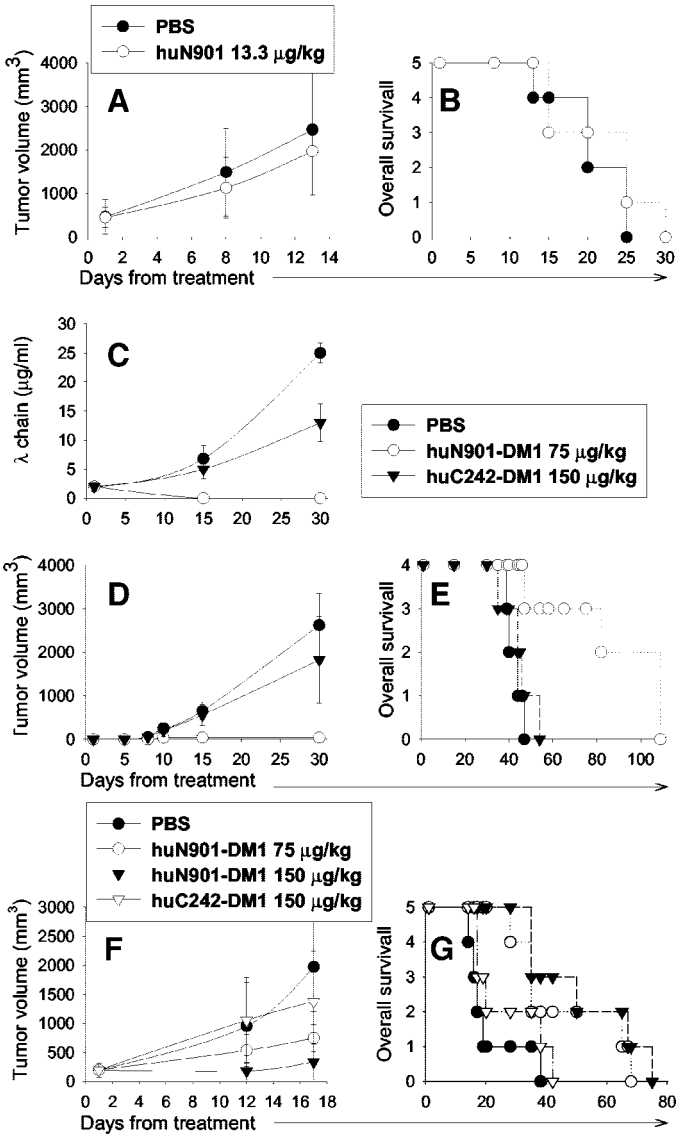

Fig. 7. Activity of huN901-DM1 in a tumor xenograft model of human CD56$^+$ MM. CB-17 SCID mice were inoculated s.c. in the interscapular area with 5×10^6 OPM2 MM cells. *A* and *B*, mice were treated i.v. with the vehicle alone (PBS) or unconjugated huN901 mAb for a total of 5 consecutive days. Tumor volume was assessed in two dimensions using an eletronic caliper every 2 weeks, and the volume was expressed in mm^3 using the formula $V = 0.5a \times b^2$, where *a* and *b* are the long and short diameter of the tumor, respectively. Tumor volume and survival were evaluated from the 1st day of treatment until day of death or sacrifice. Animals were sacrificed when their tumors reached 2 cm in diameter. *C*, *D*, and *E*, mice with minimal disease, defined as detectable human λ chain in serum without palpable tumors, were treated with vehicle alone or huN901-DM1 (75 μg/kg) or huC242-DM1 (150 μg/kg) for a total of 5 consecutive days beginning when human λ chain was detectable. Human λ chain levels were measured every 2 weeks. Tumor size (*D*) and survival (*E*) were evaluated as described above. *F* and *G*, huN901-DM1 was also studied in bulky disease. Mice were treated with huN901-DM1 (75 and 150 μg/kg) or huC242-DM1 (150 μg/kg) for 5 days (3 consecutive days followed by once a week for 2 consecutive weeks) beginning when tumor sizes reached an average of 200 mm^3. Tumor size (*F*) and survival (*G*) were evaluated as described above.

of 1:20. These mixed populations of cells were exposed to huN901-DM1 (200 nM) for 72 h and analyzed by flow cytometry. As seen in Fig. 4, *A* and *B*, huN901-DM1 induced specific depletion of CD56$^+$ cells. Compared with control, huN901-DM1 caused 3- and 5-fold reduction in the CD56$^+$/CD56$^-$ cell ratio in cultures of OPM2 with SUDHL-4 and WSU-WM cells, respectively (Fig. 4*C*), confirming selective activity of huN901-DM1 against CD56$^+$ cells.

HuN901-DM1 Induces Apoptosis of CD56$^+$ MM Cell Lines. To investigate whether apoptotic cell death occurs in cells exposed to huN901-DM1, CD56$^+$ (OPM2 and U266) and CD56$^-$ (LP1) MM cells were incubated with huN901-DM1 (100 nM) for 48 h. Apoptotic cell death was then measured by staining with annexin V and PI and flow cytometric analysis. As shown in Fig. 5, a significant increase in both annexin V$^+$/PI$^-$ and annexin V$^+$/PI$^+$ fractions was observed in CD56$^+$ cells exposed to huN901-DM1, whereas no such changes were observed for the CD56$^-$ cells. These observations confirm selective apoptotic cell death in CD56$^+$ cells after treatment with huN901-DM1.

HuN901-DM1 Induces Cell Cycle Arrest in the G_2-M Phase in CD56$^+$ OPM2 Cells. Because maytansine acts by suppressing microtubule polymerization, we next analyzed the cell cycle distribution changes induced by huN901-DM1 in CD56$^+$ OPM2 MM cells. Cells were exposed to the immunoconjugate for 48 h, labeled with PI, and analyzed on a flow cytometer. As shown in Fig. 6, mAb alone had no significant effect on the percentage of cells in G_2-M phase compared with control (21% *versus* 18%); however exposure of MM cells to huN901-DM1 induced a marked increase in the percentage of cells in the G_2-M phase (34%). DM1 alone induced a dramatic shift of cells to the G_2-M phase (84%). The difference in the extent of the cell cycle arrest induced by huN901-DM1 and free DM1 is likely due to the different rates of cell killing by the free drug and by the drug linked to a mAb, as suggested by the results shown in Fig. 2, *B* and *C*.

***In Vivo* Effects of huN901-DM1 in a MM Xenograft Model in SCID Mice.** We used a human MM xenograft model in SCID mice to study the *in vivo* activity of huN901-DM1 against CD56$^+$ tumor cells. As shown in Fig. 7, unconjugated huN901 alone (13.3 μg/kg; $n = 5$), as compared with vehicle alone (PBS; $n = 5$), had no significant effect on tumor growth (Fig. 7*A*) or survival (Fig. 7*B*), indicating that huN901 alone is not effective against CD56$^+$ MM cells.

We then studied the effect of huN901-DM1 in the MM xenograft model in both a minimal disease (undetectable s.c. disease) or bulky disease setting (large s.c. tumors). In the former study, treatment began when all animals, after tumor cell implantation, had detectable human serum paraprotein specific for the cell line injected (λ chain, average 2.2 μg/ml) without palpable tumors. Mice received i.v. injections daily for 5 days of huN901-DM1 (75 μg DM1/kg; $n = 4$), or control huC242-DM1, which does not bind OPM2 cells (150 μg DM1/kg; $n = 4$), or vehicle alone (PBS; $n = 4$). Change in serum paraprotein concentrations, development of s.c. tumors, and survival were monitored. As shown in Fig. 7*C*, reduction in serum paraprotein was observed in animals treated with huN901-DM1 after treatment for 15 days, whereas increasing levels of λ chain were detected in both control groups. In contrast, concentrations of human κ chain, comprising the injected antibody, were unaffected in both huN901-DM1 or huC242-DM1 treatment cohorts (data not shown). Palpable tumors developed in control groups 24 ± 3 days after MM cell injection (Fig. 7*D*), with progressive increase in tumor volume thereafter, whereas no tumor growth was detected in animals treated with huN901-DM1. As seen in Fig. 7*E* and as expected from serum and tumor growth results, a significant prolongation in survival was observed in mice treated with huN901-DM1 ($P < 0.001$).

We next evaluated the therapeutic efficacy of huN901-DM1 in mice bearing a significant tumor burden by starting treatment only after palpable tumors had developed (average size 200 mm^3). Animals were treated with huN901-DM1 (75 μg DM1/kg or 150 μg DM1/kg; $n = 10$), huC242-DM1 (150 μg DM1/kg; $n = 5$), or vehicle alone (PBS; $n = 5$), daily i.v. for the first 3 days and then weekly for 2 consecutive weeks. Tumor sizes and overall survival were monitored in this model. As shown in Fig. 7*F*, treatment with 75 μg/kg huN901-DM1 induced a significant delay in tumor growth, and 150 μg/kg huN901-DM1 completely inhibited tumor growth. A significant in-

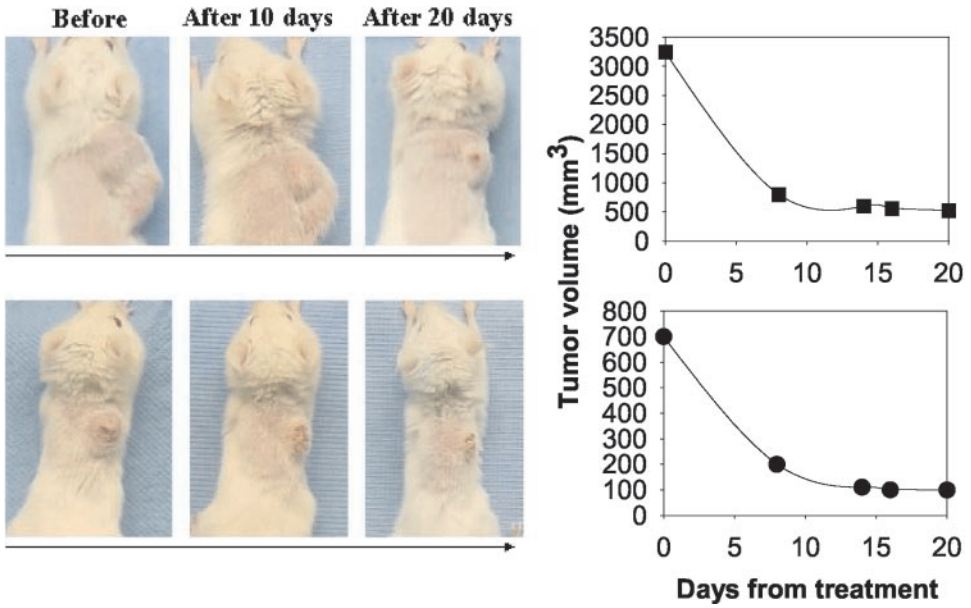

Fig. 8. Tumor regressions in mice bearing large tumors. Mice after inoculation of OPM2 MM cells were treated for 4 days with huN901-DM1 (200 μg DM1/kg). The tumor volume was measured in two dimensions using a caliper, and the volume was expressed in mm^3 using the formula $V = 0.5a \times b^2$, where a and b are the long and short diameter of the tumor, respectively.

crease in survival was observed in mice treated at both dose levels ($P < 0.001$; Fig. 7*G*).

Finally, we extended the study to even larger tumors. Two mice bearing larger MM xenografts (average size was 1800 mm^3) were treated with one course of huN901-DM1 (200 μg DM1/kg) for 4 days. As seen in Fig. 8, significant tumor regression was induced by huN901-DM1 treatment. Taken together, these results indicate that huN901-DM1 is highly active in controlling tumor growth in a murine xenograft model of human MM.

DISCUSSION

MM remains an incurable PC malignancy despite advances in systemic and supportive treatments (40–43), indicating a need for new treatments. Recently, there has been a resurgence of interest in mAb-based strategies due to approval of some mAbs for clinical use, however, to date no such treatments are available for MM.

CD56 is expressed on MM cells and not on normal PCs. We found that CD56 is expressed at high MFI on MM cells in approximately 78% of MM patients at diagnosis. These results confirm previous reports of CD56 expression on >70% of cases, assessed by flow cytometric analysis (31) as well as immunohistochemistry (32). We also confirmed high levels of expression of CD56 in MM by gene profiling. Taken together, these data confirm the potential utility of CD56 as a target antigen for immunotherapeutic approaches in MM. An important issue is the pattern of CD56 expression in normal cells: In the hematopoietic compartment, CD56 is restricted to NK cells and a subset of T lymphocytes (24, 25) and is not expressed on the majority of peripheral blood lymphocytes, monocytes, granulocytes, and RBCs. Importantly, CD56 is not expressed on $CD34^+$ hematopoietic stem cells. In nonhematopoietic compartments, CD56 is expressed on neural tissue, embryonic tissues (44), and smooth muscle (45).

The success of CD20-, CD52-, and CD33-targeted serotherapies has led to a resurgence of interest in developing mAb-based cancer treatments. Early attempts at using mAbs to deliver cytotoxic drugs were not successful, because these immunoconjugates were less active than unconjugated drugs, mainly due to the moderate cytotoxic potential of common chemotherapeutic agents. Although mAbs conjugated to toxins retained higher cytotoxic potential, these immunotoxins had systemic side effects, a narrow therapeutic index, fast clearance from the blood and high immunogenicity. The use of mAbs conjugated to the highly potent maytansine derivative, as evaluated in this study, has the advantage of significant activity and limited systemic toxicity, because the drug is not toxic while conjugated to the antibody and is released in an active form only when incorporated by target cells. An immunoconjugate of DM1 with huC242 (huC242-DM1; Refs. 21 and 46), a mAb against a glycotope on MUC1, has been recently evaluated in chemotherapy-refractory cancer patients in a Phase I clinical study (22). This study confirmed tumor localization, biological activity, and absence of severe systemic or hematological toxicity. These results provide an additional basis for evaluation of DM1 immunoconjugates in MM.

HuN901-DM1 belongs to a new generation of immunoconjugates with high activity and specificity against target cells, combined with favorable pharmacokinetics. In our study, huN901-DM1 showed both *in vitro* and *in vivo* activity against $CD56^+$ MM cells. Selective activity of huN901-DM1 against target cells was also confirmed in cocultures of $CD56^+$ and $CD56^-$ cells and on patient MM cells. Importantly, treatment with huN901-DM1 in our tumor xenograft model of human MM was effective in both a minimal and a bulky disease setting. In contrast, no therapeutic effect was observed by injection of equimolar or higher doses of isotype-matched control immunoconjugate huC242-DM1, which does not react with $CD56^+$ tumors.

CD56 has been previously evaluated as a therapeutic target in SCLC using the murine mAb N901 conjugated with blocked ricin (bR; Ref. 47). The immunoconjugate N901-bR showed potent cytotoxicity against $CD56^+$ SCLC cells in preclinical studies. Importantly, in a Phase I study treating patients with relapsed SCLC, N901-bR was well tolerated with acceptable toxicity (48) and potential clinical activity. In addition, immunohistochemical staining of tissue samples from patients receiving infusion of N901-bR has demonstrated the selective binding of the immunotoxin to target tumor SCLC cells located in the BM and other tissues (48). This study suggested that mAb N901 linked to a cytotoxic agent can recognize and target $CD56^+$ tumor cells *in vivo*, in particular in a setting of a disseminated human disease involving BM localization.

In conclusion, huN901-DM1 represents a new generation of immunoconjugates with activity in a preclinical model of MM. The current data provide the *in vitro* and *in vivo* preclinical framework for evaluation of huN901-DM1 therapy to improve patient outcome in MM.

REFERENCES

1. Carter P. Improving the efficacy of antibody-based cancer therapies. Nat Rev Cancer 2001;1:118–29.
2. Dillman RO. Monoclonal antibodies in the treatment of malignancy: basic concepts and recent developments. Cancer Invest 2001;19:833–41.
3. Maloney DG, Grillo-Lopez AJ, White CA, et al. IDEC-C2B8 (Rituximab) anti-CD20 monoclonal antibody therapy in patients with relapsed low-grade non-Hodgkin's lymphoma. Blood 1997;90:2188–95.
4. Leget GA, Czuczman MS. Use of rituximab, the new FDA-approved antibody. Curr Opin Oncol 1998;10:548–51.
5. Schwartzberg LS. Clinical experience with edrecolomab: a monoclonal antibody therapy for colorectal carcinoma. Crit Rev Oncol Hematol 2001;40:17–24.
6. Farah RA, Clinchy B, Herrera L, Vitetta ES. The development of monoclonal antibodies for the therapy of cancer. Crit Rev Eukaryotic Gene Expression 1998;8: 321–56.
7. Trail PA, Willner D, Lasch SJ, et al. Cure of xenografted human carcinomas by BR96-doxorubicin immunoconjugates. Science 1993;261:212–5.
8. Kanellos J, Pietersz GA, McKenzie IF. Studies of methotrexate-monoclonal antibody conjugates for immunotherapy. J Natl Cancer Inst (Bethesda) 1985;75:319–32.
9. Starling JJ, Maciak RS, Law KL, et al. In vivo antitumor activity of a monoclonal antibody-Vinca alkaloid immunoconjugate directed against a solid tumor membrane antigen characterized by heterogeneous expression and noninternalization of antibody-antigen complexes. Cancer Res 1991;51:2965–72.
10. Pastan I. Targeted therapy of cancer with recombinant immunotoxins. Biochim Biophys Acta 1997;1333:C1–6.
11. Bross PF, Beitz J, Chen G, et al. Approval summary: gemtuzumab ozogamicin in relapsed acute myeloid leukemia. Clin Cancer Res 2001;7:1490–6.
12. Hamann PR, Hinman LM, Beyer CF, et al. An anti-CD33 antibody-calicheamicin conjugate for treatment of acute myeloid leukemia: choice of linker. Bioconjug Chem 2002;13:40–6.
13. Dowell JA, Korth-Bradley J, Liu H, King SP, Berger MS. Pharmacokinetics of gemtuzumab ozogamicin, an antibody-targeted chemotherapy agent for the treatment of patients with acute myeloid leukemia in first relapse. J Clin Pharmacol 2001;41: 1206–14.
14. Remillard S, Rebhun LI, Howie GA, Kupchan SM. Antimitotic activity of the potent tumor inhibitor maytansine. Science 1975;189:1002–5.
15. Chabner BA, Levine AS, Johnson BL, Young RC. Initial clinical trials of maytansine, an antitumor plant alkaloid. Cancer Treat Rep 1978;62:429–33.
16. Blum RH, Kahlert T. Maytansine: a Phase I study of an ansa macrolide with antitumor activity. Cancer Treat Rep 1978;62:435–8.
17. Cabanillas F, Rodriguez V, Hall SW, Burgess MA, Bodey GP, Freireich EJ. Phase I study of maytansine using a 3-day schedule. Cancer Treat Rep 1978;62:425–8.
18. Issell BF, Crooke ST. Maytansine. Cancer Treat Rev 1978;5:199–207.
19. Chari RV, Martell BA, Gross JL, et al. Immunoconjugates containing novel maytansinoids: promising anticancer drugs. Cancer Res 1992;52:127–31.
20. Haglund C, Lindgren J, Roberts PJ, Kuusela P, Nordling S. Tissue expression of the tumour associated antigen CA242 in benign and malignant pancreatic lesions: a comparison with CA 50 and CA 19-9. Br J Cancer 1989;60:845–51.
21. Liu C, Tadayoni BM, Bourret LA, et al. Eradication of large colon tumor xenografts by targeted delivery of maytansinoids. Proc Natl Acad Sci USA 1996;93:8618–23.
22. Tolcher AW, Ochoa L, Hammond LA, et al. Cantuzumab mertansine, a maytansinoid immunoconjugate directed to the CanAg antigen: a Phase I, pharmacokinetic, and biologic correlative study. J Clin Oncol 2003;21:211–22.
23. Thiery JP, Brackenbury R, Rutishauser U, Edelman GM. Adhesion among neural cells of the chick embryo. II. Purification and characterization of a cell adhesion molecule from neural retina. J Biol Chem 1977;252:6841–5.
24. Lanier LL, Le AM, Civin CI, Loken MR, Phillips JH. The relationship of CD16 (Leu-11) and Leu-19 (NKH-1) antigen expression on human peripheral blood NK cells and cytotoxic T lymphocytes. J Immunol 1986;136:4480–6.
25. Schmidt RE, Murray C, Daley JF, Schlossman SF, Ritz J. A subset of natural killer cells in peripheral blood displays a mature T cell phenotype. J Exp Med 1986;164: 351–6.
26. Lanier LL, Chang C, Azuma M, Ruitenberg JJ, Hemperly JJ, Phillips JH. Molecular and functional analysis of human natural killer cell- associated neural cell adhesion molecule (N-CAM/CD56). J Immunol 1991;146:4421–6.
27. Griffin JD, Hercend T, Beveridge R, Schlossman SF. Characterization of an antigen expressed by human natural killer cells. J Immunol 1983;130:2947–51.
28. Patel K, Moore SE, Dickson G, et al. Neural cell adhesion molecule (NCAM) is the antigen recognized by monoclonal antibodies of similar specificity in small-cell lung carcinoma and neuroblastoma. Int J Cancer 1989;44:573–8.
29. Harada H, Kawano MM, Huang N, et al. Phenotypic difference of normal plasma cells from mature myeloma cells. Blood 1993;81:2658–63.
30. Rawstron AC, Owen RG, Davies FE, et al. Circulating plasma cells in multiple myeloma: characterization and correlation with disease stage. Br J Haematol 1997; 97:46–55.
31. Sahara N, Takeshita A, Shigeno K, et al. Clinicopathological and prognostic characteristics of CD56-negative multiple myeloma. Br J Haematol 2002;117:882–5.
32. Ely SA, Knowles DM. Expression of CD56/neural cell adhesion molecule correlates with the presence of lytic bone lesions in multiple myeloma and distinguishes myeloma from monoclonal gammopathy of undetermined significance and lymphomas with plasmacytoid differentiation. Am J Pathol 2002;160:1293–9.
33. Pellat-Deceunynck C, Barille S, Puthier D, et al. Adhesion molecules on human myeloma cells: significant changes in expression related to malignancy, tumor spreading, and immortalization. Cancer Res 1995;55:3647–53.
34. Pellat-Deceunynck C, Barille S, Jego G, et al. The absence of CD56 (NCAM) on malignant plasma cells is a hallmark of plasma cell leukemia and of a special subset of multiple myeloma. Leukemia 1998;12:1977–82.
35. Lust JA, Donovan KA. Biology of the transition of monoclonal gammopathy of undetermined significance (MGUS) to multiple myeloma. Cancer Control 1998;5: 209–17.
36. Kaiser U, Auerbach B, Oldenburg M. The neural cell adhesion molecule NCAM in multiple myeloma. Leuk Lymphoma 1996;20:389–95.
37. Roguska MA, Pedersen JT, Keddy CA, et al. Humanization of murine monoclonal antibodies through variable domain resurfacing. Proc Natl Acad Sci USA 1994;91: 969–73.
38. Mosmann T. Rapid colorimetric assay for cellular growth and survival: application to proliferation and cytotoxicity assays. J Immunol Methods 1983;65:55–63.
39. Jego G, Robillard N, Puthier D, et al. Reactive plasmacytoses are expansions of plasmablasts retaining the capacity to differentiate into plasma cells. Blood 1999;94: 701–12.
40. Hideshima T, Richardson P, Anderson KC. Novel therapeutic approaches for multiple myeloma. Immunol Rev 2003;194:164–76.
41. Anderson KC. Moving disease biology from the lab to the clinic. Cancer 2003; 97(Suppl):796–801.
42. Munshi NC, Hideshima T, Chauhan D, Richardson P, Anderson KC. Novel biologically based therapies for multiple myeloma. Int J Hematol 2002;76(Suppl 1):340–1.
43. Hideshima T, Anderson KC. Molecular mechanisms of novel therapeutic approaches for multiple myeloma. Nat Rev Cancer 2002;2:927–37.
44. Crossin KL, Chuong CM, Edelman GM. Expression sequences of cell adhesion molecules. Proc Natl Acad Sci USA 1985;82:6942–6.
45. Akeson RA, Wujek JR, Roe S, Warren SL, Small SJ. Smooth muscle cells transiently express NCAM. Brain Res 1988;464:107–20.
46. Smith S. Technology evaluation: C242-DM1, ImmunoGen Inc. Curr Opin Mol Ther 2001;3:198–203.
47. Epstein C, Lynch T, Shefner J, et al. Use of the immunotoxin N901-blocked ricin in patients with small-cell lung cancer. Int J Cancer Suppl 1994;8:57–9.
48. Lynch TJ Jr, Lambert JM, Coral F, et al. Immunotoxin therapy of small-cell lung cancer: a Phase I study of N901-blocked ricin. J Clin Oncol 1997;15:723–34.